European Journal of Sustainable Development (2024), **13**, 4, 467-476 ISSN: 2239-5938
Doi: 10.14207/ejsd.2024.v13n4p467

Impacts on Biogenic Carbon Dioxide Emission Fluxes Driven by Generated Numerical-Downscaled Climate Scenarios

By Roberto San Jose[1], J. L. Perez-Camanyo1 and Miguel Jiménez Gañan[1]

ABSTRACT:
The aim of this research is to analyze the local impacts (high spatial resolution) of tier 1 CMIP6 climate scenarios (SSP126, SSP245, SSP370 and SSP585) on CO2 biogenic emission fluxes after downscaled climate data over five European regions (national, regional and urban scale) for the period: 2015-2050 using numerical simulations with the WRF/Chem-VPRM tool. VPRM is the Vegetation Photosynthesis and Respiration Model which is coupled with the Weather Research and Forecasting (WRF) model and Chem (Transport). Satellite data is used to derive vegetation indexes used by the VPRM model. The effect of climate is isolated using 2018 (reference year) emissions and land use over the entire simulation period and it is calculated as results of the future simulations minus present (2018). The research is part of the European DISTENDER project, who develops a methodological framework to bring together adaptation and mitigation strategies against the risks of climate change. The increase in temperature leads to higher CO2 emissions from vegetation, as the increase in temperature favors the respiration process of plants. The impacts are spatially and temporally varied and therefore each case study and scenario has its own pattern, with a strong influence on the existing vegetation and local climate.

Keywords: Climate change, CO2, biogenic emissions, scenarios, downscaling

1. Introduction

Carbon dioxide (CO2) is the primary anthropogenic greenhouse gas driving climate change. Understanding carbon sources and sinks is crucial for addressing global warming (IPCC, 2022). The Paris Agreement mandates significant CO2 emission reductions, with many cities targeting net zero emissions by 2050. Accurate quantification and monitoring of emissions are critical (Bezyk et al., 2021; Lei & Han, 2020; McHale et al., 2017). CO2 fluxes by vegetation vary widely, impacting atmospheric concentrations and introducing tracking uncertainties (Miller et al., 2020). Comprehensive assessments of CO2 fluxes are essential for cities pursuing carbon neutrality. While global climate models (GCMs) offer broad-scale data, regional climate models (RCMs) provide finer insights, especially in complex terrains. The latest IPCC report highlights the need for high-resolution regional data. The 6th phase of the Coupled Model Intercomparison Project (CMIP6) includes extensive GCMs based on various greenhouse gas emission scenarios (Shared Socio-Economic Pathways, SSPs). GCMs' coarse resolution necessitates dynamic downscaling with RCMs for detailed regional analysis. Dynamical downscaling offers

[1]Environmental Software and Modelling Group, Computer Science School, Technical University of Madrid (UPM), Madrid, Spain.

significant advantages in providing high-resolution climate signals that global models often lack, especially when it comes to capturing the complexities of local terrain, microclimates and fine-scale atmospheric processes. Such detailed knowledge is essential to accurately predict CO2 fluxes, especially in regions with diverse topography and land use. One of the limitations of this technique is that it often relies on boundary conditions set by global models, which may still have uncertainties. This study uses the Weather Research and Forecasting (WRF) model to downscale CMIP6 data, providing high-resolution climate signals for five European regions. High-resolution simulations with the WRF/Chem-VPRM model will quantify CO2 sources and sinks, focusing on advection and diffusion of biogenic CO2 fluxes without chemical reactions due to CO2's long atmospheric lifetime (Dekker et al., 2017). The WRF/Chem-VPRM model has proven effective in studying CO2 fluxes (Dong et al., 2021), but its high-resolution application to future climate scenarios remains unexplored. This research aims to analyze biogenic CO2 flux responses to climate scenarios from 2015-2050 across five European regions.

This research, part of the EU-funded DISTENDER project coordinated by UPM, aims to integrate adaptation and mitigation strategies using participatory approaches to address climate change impacts and risks. DISTENDER combines quantitative and qualitative analyses to understand interactions, synergies, and trade-offs. The project emphasizes flexible, participatory planning tailored to specific contexts for effective mitigation and adaptation. DISTENDER will develop multi-factor socio-economic and climate scenarios through a participatory process, integrating local knowledge with broader information. These methodologies will be applied in five main case studies at various scales and six complementary case studies. The project will provide a decision support system (DSS) to help policymakers select appropriate strategies for identified climate risks.

2. Experiment

The numerical modelling system is used to simulate CO_2 fluxes and atmospheric CO_2 concentrations over five European regions corresponding to the five cases studies of the DISTENDER project. The table 1 shows the five experiments.

The modelling approach uses a bidirectional nesting technique in the cases studies with multiple domains. Each domain has 33 vertical layers extending from the surface down to 10 hPa. The simulation period spans from 2015 to 2050. The WRF/Chem-VPRM downscaling simulation runs continuously from 1 January to 31 December each year, with a one-day turnaround period. We generated hourly outputs over 35 years for four climate scenarios and three domains. Initial and boundary weather conditions, updated every six hours, are sourced from the MPI-ESM1-2-HR climate model outputs. This model is selected for its favorable features, including a well-balanced radiation budget and an explicit climate sensitivity tuned to 3 ºK, as detailed by Müller et al. (2018), making it particularly suitable for predictive modeling and impact assessments. MPI-ESM1-2-HR operates with a horizontal grid spacing of approximately 100 km in the atmosphere and 40 km in the ocean, as specified by Mauritsen et al. (2019).

The climate model outputs require interpolation to align with the WRF grid configuration. This task is performed using the CMIP6-to-WRFInterim tool, which

employs a pure Python implementation to convert CMIP6 sub-daily outputs into WRF intermediate files, which serve as inputs to drive the WRF model in regional dynamic downscaling applications. The CMIP6-to-WRFInterim tool is available at https://github.com/lzhenn/cmip6-to-wrfinterm. Four CMIP6 global scenario simulations SSP1-2.6, SSP2-4.5, SSP3-7.0 and SSP5-8.5 (Eyring et al., 2016; O'Neill et al., 2016) developed by the MPI-ESM1.2-HR model have been rescaled.

Table 1. Case studies and computational domains.

Identifier	Case study	Scale	Domains
Austria	Federal Ministry For Climate Protection, Environment, Energy, Mobility, Innovation And Technology (BMK)	National	D1: 40 x 20 grid cells by 20 km.
HUAS	North-east of The Netherlands The Netherland Water Management Authority represented by Hanze University	Regional	D1: 30 x 20 grid cells by 27 km. D2: 30 x 30 grid cells by 9 km.
EURAF	South-West Iberian Peninsula, Dehesa-Montado represented **by** European Agroforestry Federation	National/regional	D1: 30 x 20 grid cells by 20 km.
CMTo	Metropolitan City of Turin in Italy	Regional/urban	D1: 30 x 30 grid cells by 21 km. D2: 30 x 30 grid cells by 7 km.
Guimaraes	City in Portugal	Urban	D1: 30 x 30 grid cells by 9 km. D2: 30 x 30 grid cells by 3 km. D3: 30 x 30 grid cells by 1 km.

3. Modelling tools

We utilize the Weather Research and Forecasting model (WRF) coupled with Chemistry version 4.5 (WRF-Chem, Grell et al., 2005). This Eulerian atmospheric transport model simulates the three-dimensional concentration of trace gases at every time step, concurrently with meteorological fields (Skamarock et al., 2019; Fast et al., 2006) in its passive tracer option. WRF-Chem is coupled with the Vegetation Photosynthesis and Respiration Model (VPRM) (Mahadevan et al., 2008; Ahmadov et al., 2007), which calculates biogenic CO_2 fluxes online. Table 2 lists the physics configuration employed in the current study. The Vegetation Photosynthesis and Respiration Model (VPRM) serves as a diagnostic parameterisation tool for CO_2 fluxes in the biosphere, using high-resolution land use data, vegetation indices from satellite observations and simulated radiation and air temperature data from the WRF.

Table 2. Physics Configuration of WRF/Chem-VPRM (San José et al., 2015)

Model Physics	Configuration
Microphysics	Morrison double-moment
Long/Short Wave Radiation	Rapid Radiative Transfer Method for Global models (RRTMG)
Planetary Boundary Layer	Yonsei University (YSU)
Surface Layer	Monin-Obukhov
Land Surface	Noah land surface model
Cumulus	Grell-3D (G3)
CO_2	Passive tracer mode

VPRM input data have associated uncertainties that affect the accuracy of model predictions. Previous studies have shown that the influence of uncertainty in meteorological data is much greater than that of land use and satellite data (Chen et al., 2020). VPRM enables accurate simulation of CO_2 uptake and release fluxes from the biosphere at high spatio-temporal resolution. VPRM works by simulating the Net Ecosystem Exchange (NEE) of CO_2 following Equation (1), which is achieved by different parameterisations for ecosystem respiration (Respiration, Equation (2)) and Gross Primary Production (GPP, Equation (3)), as described in Mahadevan et al., 2008.

$$NEE = -GPP + Respiration \quad (1)$$

$$Respiration = \alpha T_{air} + \beta \quad (2)$$

$$GPP = (\lambda T_S W_s P_s) FAPAR_{PAV} \frac{1}{1+\frac{PAR}{PAR_0}} PAR \quad (3)$$

- α and β are respiration parameters associated with the eight vegetation classes of VPRM optimized for the European domains (Hilton et al. 2013).
- Tair is the air temperature,
- λ, Ts, Ws,Ps are parameters which depends of the air temperature and the Land Surface Water Index (LSWI).
- FAPARPAV is the fraction of absorbed photosynthetically active radiation (PAR), and it roughly equates to the Enhanced Vegetation Index (EVI). PAR is derived (0.505) from the short wave radiation of the WRF.

EVI and LSWI are aggregated from MODIS surface reflectance 8d L3 Global 500 m (MOD09A1) version 6 data, 500 m spatial resolution with 8 days frequency. Anthropogenic CO_2 emission were calculated with the EMIMO Emission Model (San Jose et al., 2015) from the CAMS-GLOB-ANT emission inventory developed as part of the Copernicus Atmosphere Monitoring Service (CAMS) with 0.1x0.1 degree of spatial resolution. 2018 is the reference year to isolate the climate signal. The VPRM reads every model time step the temperature and the shortwave downward radiation produced by the WRF model. VPRM calculates biogenic fluxes of CO_2 to be transported/dispersed by the Chem part of the WRF/Chem model. The transport and dispersion require winds and

turbulence atmospheric parameters which are simulated by the WRF model (Ahmadov et al., 2007).

4. Results

The modeling tool described above produces multiple output variables. For this study, the analyzed variables include air temperature (in Kelvin) at 2 meters altitude, CO_2 vegetation fluxes (Kmol km^-1 hr^-1) referred to as BUDGET, and CO_2 concentrations (ppm). The analysis focuses on these variables due to their relevance in understanding the impacts of climate change and the effectiveness of mitigation strategies. To isolate the climate impact, we have generated maps of the mean differences between each year (2019, 2020, ..., 2050) and the reference year 2018. These maps highlight changes over time, with negative values indicating an improvement in fluxes (which can be positive when emitting or negative when absorbing) and positive values indicating a worsening, either through increased emissions or reduced removals. The BUDGET maps for each case study under different socio-economic and climate scenarios illustrate the results of the study. These maps provide a visual representation of how CO_2 fluxes are expected to change over time under varying conditions. Specifically, the following figures depict the results: Figure 1 is Austria for SSP126, Figure 2 is EURAF for SSP370, Figure 3 is HUAS for SSP126, Figure 4 is CMTo for SSP245 and Figure 5 is Guimaraes for SSP370.

Figure 1 illustrates contrasting CO_2 biogenic flux trends between Western and Eastern regions. In the West, rising temperatures worsen fluxes, increasing emissions or reducing CO_2 absorption, thereby raising atmospheric CO_2.

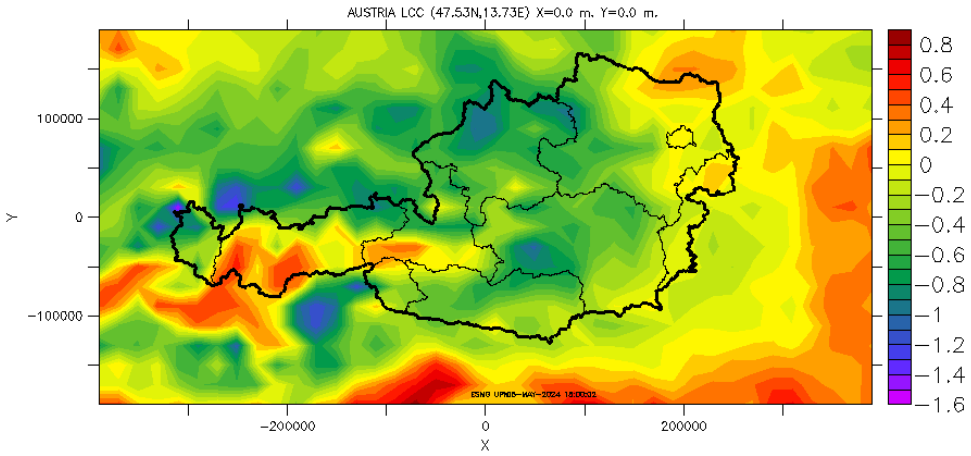

Figure 1: Austria case study, map of the BUDGET (Km km-2 hr-1) average differences between 2019 to 2050 minus 2018 for the SSP126 scenario.

The East shows slight improvements in fluxes, especially from 2040-2050, but these gains are insufficient to counteract Western deterioration, highlighting the need for regional mitigation strategies. Temporal analysis from 2019-2050 shows a worsening trend in Western fluxes due to ongoing temperature rises, while Eastern regions, despite resilience, cannot fully offset Western impacts.

Figure 2 depicts the SSP370 scenario's impact on CO_2 biogenic fluxes, showing improvements due to decreased temperatures enhancing vegetation's CO_2 absorption via efficient photosynthesis and respiration. However, changes in CO_2 concentrations remain minor, suggesting other influencing factors like anthropogenic emissions and atmospheric transport. The improvements in biogenic fluxes under SSP370 highlight natural systems' climate mitigation potential, but modest CO_2 concentration changes emphasize the carbon cycle's complexity. Temporal analysis within SSP370 indicates stable biogenic flux improvements, implying sustained carbon absorption if favorable conditions persist.

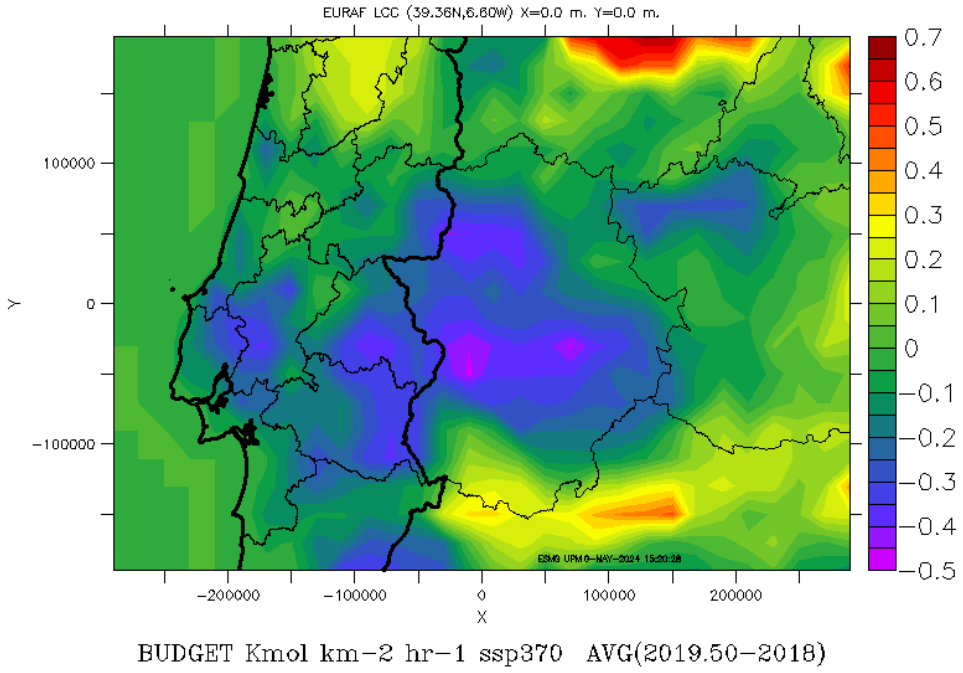

Figure 2: EURAF case study, map of the BUDGET (Km km-2 hr-1) average differences between 2019 to 2050 minus 2018 for the SSP370 scenario.

Figure 3 demonstrates the heterogeneous impact of the SSP126 scenario on CO_2 biogenic fluxes and concentrations across the domain. The spatial distribution reveals localized positive and negative effects, reflecting varied responses to climate change factors like temperature, precipitation, and vegetation dynamics. Regions with favorable conditions show significant improvements in biogenic fluxes, enhancing carbon absorption and reducing CO_2 concentrations, highlighting the effectiveness of low-

emission pathways. However, areas with adverse factors experience deteriorating fluxes, emphasizing the need for tailored climate strategies. While SSP126 shows overall positive trends, targeted interventions are essential to address localized challenges and ensure comprehensive climate resilience and mitigation

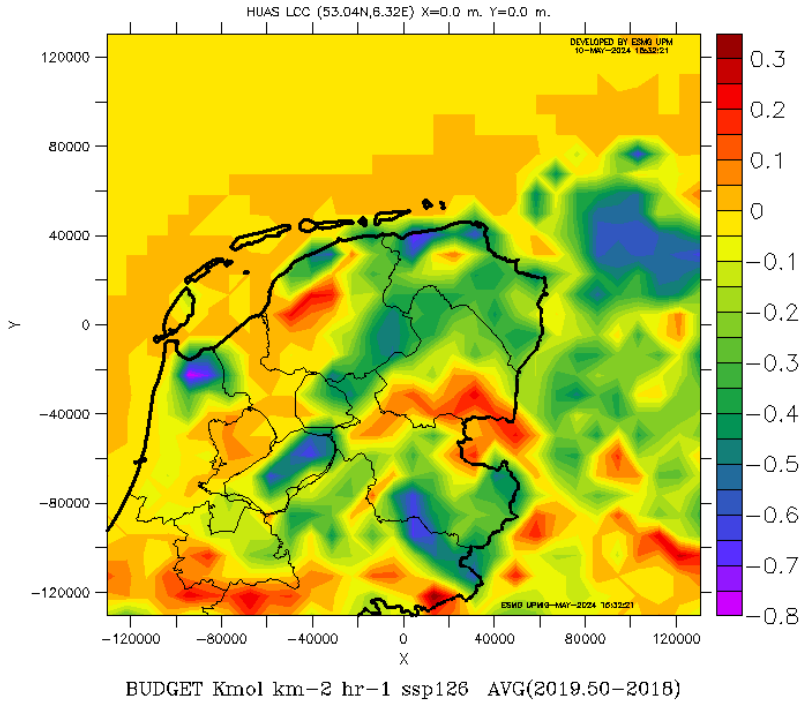

Figure 3: HUAS case study, map of the BUDGET (Km km-2 hr-1) average differences between 2019 to 2050 minus 2018 for the SSP126 scenario.

Figure 4 depicts a general decline in biogenic CO_2 fluxes across the study area, indicating increased emissions or reduced vegetation absorption under future scenarios due to adverse climatic conditions like rising temperatures and altered precipitation patterns. Despite the negative trend, some areas show improvements in biogenic fluxes, possibly due to local factors like microclimates or resilient vegetation. However, the eastern region of Turin exhibits significant increases in CO_2 concentrations and air temperature, indicating a substantial decrease in carbon sequestration capacity. These findings highlight the urgency of targeted climate strategies, especially in regions like east Turin, to mitigate worsening biogenic fluxes and rising CO_2 concentrations effectively.

Figure 5 demonstrates minimal impacts on biogenic CO_2 emission fluxes and air temperature, accompanied by a decrease in CO_2 concentrations. The slight changes in biogenic fluxes suggest that the region's vegetation and land management practices maintain a stable balance between carbon absorption and emissions despite potential climatic variations. This stability may be attributed to adaptive vegetation types or effective land management strategies that mitigate climate change impacts.

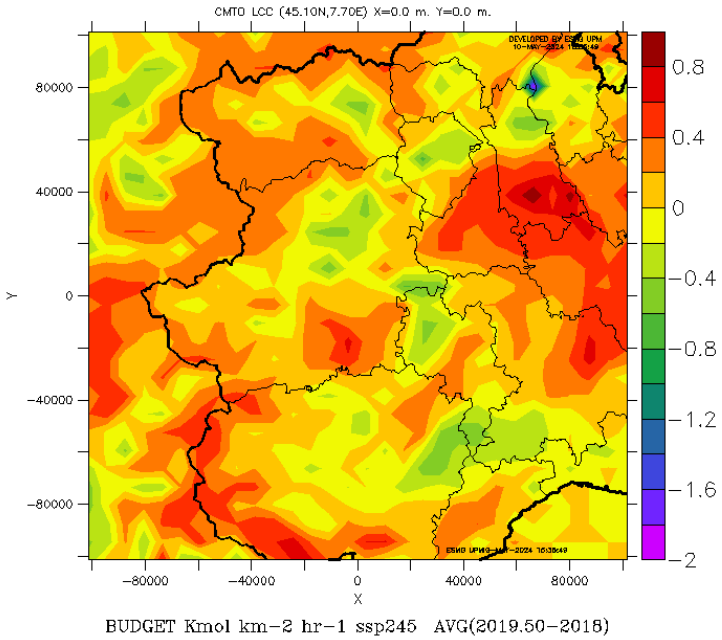

Figure 4: CMTo case study, map of the BUDGET (Km km-2 hr-1) average differences between 2019 to 2050 minus 2018 for the SSP245 scenario.

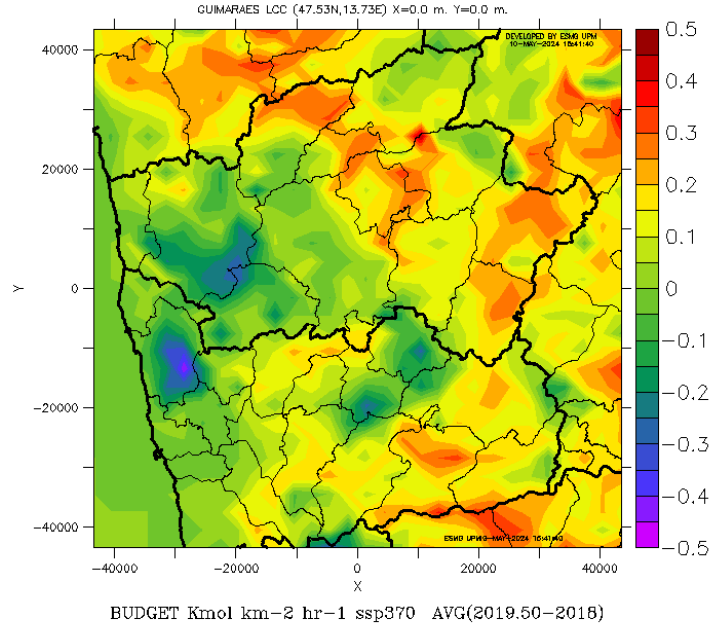

Figure 5: Guimaraes case study, map of the BUDGET (Km km-2 hr-1) average differences between 2019 to 2050 minus 2018 for the SSP370 scenario.

5. Conclusion

A general increase in temperature is observed in all scenarios and case studies. Although the SSP3 scenario in Austria, EURAF and GUIMARAES shows decreases in temperature. The largest increases are expected in CMTo and the smallest in HUAS. The increase in temperature in this scenarios leads to higher CO_2 emissions from vegetation, as the increase in temperature favours the respiration process of plants. The impacts on biogenic CO_2 emission fluxes are spatially and temporally varied and therefore each case study and scenario has its own pattern, with a strong influence on the existing vegetation. CO_2 concentrations tend to increase in Austria, EURAF and CMTO, with the largest expected increases. They decrease slightly in HUAs and GUIMARES. In many areas there are improvements in biogenic emission fluxes but CO_2 concentrations continue to increase as concentrations are affected by boundary conditions and CO_2 transport.

The results show that different regions and vegetation types respond uniquely to climate change. For example, in some areas CO2 uptake may increase, while in others carbon sequestration may decrease due to temperature changes. Analyzing local climate and vegetation influences allows for more accurate and effective mitigation strategies. It ensures that interventions are tailored to the context and address the unique challenges and opportunities presented by each region.

The development of adaptive vegetation management practices tailored to specific regions could substantially improve carbon sequestration. These practices may include optimising land use, selecting appropriate plant species that are resilient to climate change, and applying conservation techniques that preserve or enhance natural carbon sinks. Furthermore, the conclusion invites further study on how these strategies can be effectively implemented, especially in diverse ecological contexts. By focusing on local impacts and carbon sequestration potential, specific climate strategies can make a significant contribution to global climate change mitigation efforts, ensuring that interventions are both scientifically sound and practically feasible.

Acknowledgment: The UPM authors acknowledge the computer resources and technical assistance provided by the Centro de Supercomputación y Visualización de Madrid (CeSViMa). The UPM authors thankfully acknowledge the computer resources, technical expertise and assistance provided by the Red Española de Supercomputación. DISTENDER has received funding from the European Union's Horizon EU research and innovation programme under grant agreement No 101056836".

References

Al-Alawi, A., Abdulmohsen, M., Al-Malki, A., & Mehrotra, A. (2019): Investigating the Barriers to Change Management in Public Sector Educational Institutions. *International Journal of Educational Management* 33(2) DOI: http://dx.doi.org/10.1108/IJEM-03-2018-0115

Ahmadov, R., Gerbig, C., Kretschmer, R., Koerner, S., Neininger, B., Dolman, A. J., & Sarrat, C. (2007). Mesoscale covariance of transport and CO2fluxes: Evidence from observations and simulations using the WRF-VPRM coupled atmosphere-biosphere model. *Journal of Geophysical Research*, *112*(D22). https://doi.org/10.1029/2007jd008552

Bezyk, Y., Sówka, I., & Górka, M. (2021). Assessment of urban CO2 budget: Anthropogenic and biogenic inputs. *Urban Climate*, *39*, 100949. https://doi.org/10.1016/j.uclim.2021.100949

Chen, J., Gerbig, C., Marshall, J., and Totsche, K. U (2020). Short-term forecasting of regional biospheric CO2 fluxes in Europe using a light-use-efficiency model (VPRM, MPI-BGC version 1.2), Geosci. Model Dev., 13, 4091–4106, https://doi.org/10.5194/gmd-13-4091-2020

Dekker, I. N., Houweling, S., Aben, I., Röckmann, T., Krol, M., Martínez-Alonso, S., Deeter, M. N., & Worden, H. M. (2017). Quantification of CO emissions from the city of Madrid using MOPITT satellite retrievals and WRF simulations. *Atmospheric Chemistry and Physics*, *17*(23), 14675–14694. https://doi.org/10.5194/acp-17-14675-2017

Dong, X., Yue, M., Jiang, Y., Hu, X.-M., Ma, Q., Pu, J., & Zhou, G. (2021). Analysis of CO₂ spatio-temporal variations in China using a weather–biosphere online coupled model. *Atmospheric Chemistry and Physics*, *21*(9), 7217–7233. https://doi.org/10.5194/acp-21-7217-2021

Eyring, V., Bony, S., Meehl, G. A., Senior, C. A., Stevens, B., Stouffer, R. J., & Taylor, K. E. (2016). Overview of the Coupled Model Intercomparison Project Phase 6 (CMIP6) experimental design and organization. *Geoscientific Model Development*, *9*(5), 1937–1958. https://doi.org/10.5194/gmd-9-1937-2016

Fast, J. D., Gustafson, W. I., Easter, R. C., Zaveri, R. A., Barnard, J. L., Chapman, E., Grell, G., & Peckham, S. E. (2006). Evolution of ozone, particulates, and aerosol direct radiative forcing in the vicinity of Houston using a fully coupled meteorology-chemistry-aerosol model. *Journal of Geophysical Research*, *111*(D21). https://doi.org/10.1029/2005jd006721

Grell, G. A., Peckham, S. E., Schmitz, R., McKeen, S. A., Frost, G., Skamarock, W. C., & Eder, B. (2005). Fully coupled "online" chemistry within the WRF model. *Atmospheric Environment*, *39*(37), 6957–6975. https://doi.org/10.1016/j.atmosenv.2005.04.027

IPCC. (2022). Climate Change 2022: Impacts, Adaptation and Vulnerability Working Group II Contribution to the Sixth Assessment Report of the Intergovernmental Panel on Climate Change. *IPCC*, *1*(1). https://doi.org/10.1017/9781009325844

Lei, N., & Han, J. (2020). Effect of precipitation on respiration of different reconstructed soils. *Scientific Reports*, *10*, 7328. https://doi.org/10.1038/s41598-020-63420-x

Mahadevan, P., Wofsy, S. C., Matross, D. M., Xiao, X., Dunn, A. L., Lin, J. C., Gerbig, C., Munger, J. W., Chow, V. Y., & Gottlieb, E. W. (2008). A satellite-based biosphere parameterization for net ecosystem CO2exchange: Vegetation Photosynthesis and Respiration Model (VPRM). *Global Biogeochemical Cycles*, *22*(2), n/a-n/a. https://doi.org/10.1029/2006gb002735

McHale, M. R., Hall, S. J., Majumdar, A., & Grimm, N. B. (2017). Carbon lost and carbon gained: a study of vegetation and carbon trade-offs among diverse land uses in Phoenix, Arizona. *Ecological Applications*, *27*(2), 644–661. https://doi.org/10.1002/eap.1472

Miller, J. B., Lehman, S. J., Verhulst, K. R., Miller, C. E., Duren, R. M., Yadav, V., Newman, S., & Sloop, C. D. (2020). Large and seasonally varying biospheric CO2 fluxes in the Los Angeles megacity revealed by atmospheric radiocarbon. *Proceedings of the National Academy of Sciences*, *117*(43), 26681–26687. https://doi.org/10.1073/pnas.2005253117

Müller, W. A., Jungclaus, J. H., Mauritsen, T., Baehr, J., Bittner, M., Budich, R., Bunzel, F., Esch, M., Ghosh, R., Haak, H., Ilyina, T., Kleine, T., Kornblueh, L., Li, H., Modali, K., Notz, D., Pohlmann, H., Roeckner, E., Stemmler, I., & Tian, F. (2018). A Higher-resolution Version of the Max Planck Institute Earth System Model (MPI-ESM1.2-HR). *Journal of Advances in Modeling Earth Systems*, *10*(7), 1383–1413. https://doi.org/10.1029/2017ms001217

O'Neill, B. C., Tebaldi, C., van Vuuren, D. P., Eyring, V., Friedlingstein, P., Hurtt, G., Knutti, R., Kriegler, E., Lamarque, J.-F., Lowe, J., Meehl, G. A., Moss, R., Riahi, K., & Sanderson, B. M. (2016). The Scenario Model Intercomparison Project (ScenarioMIP) for CMIP6. *Geoscientific Model Development*, *9*(9), 3461–3482. https://doi.org/10.5194/gmd-9-3461-2016

San Jose, R., Mercado Pérez J., Balzarini, A., Baró R., Curci G, Forkel, R., Galmarini S., Grell, G., Hirtl, M., Honzak L., Im, U., Jiménez-Guerrero, P., Langer, M., Pirovano G., Tuccella P., Werhahn, J. C., & Žabkar R.. (2015). Sensitivity of feedback effects in CBMZ/MOSAIC chemical mechanism. *Atmospheric Environment*, *115*, 646–656. https://doi.org/10.1016/j.atmosenv.2015.04.030

Skamarock, C., Klemp, B., Dudhia, J., Gill, O., Liu, Z., Berner, J., Wang, W., Powers, G., Duda, G., Barker, D., & Huang, X. (2019). A Description of the Advanced Research WRF Model Version 4. *Opensky.ucar.edu*. https://doi.org/10.5065/1dfh-6p97